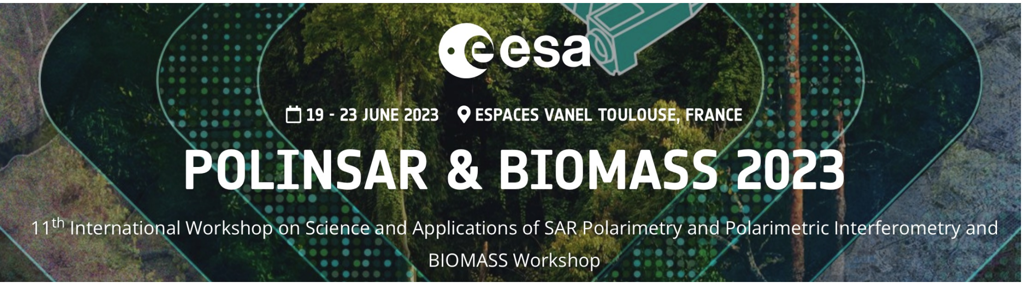

SNOW WATER EQUIVALENT RETRIEVAL USING SPACEBORNE REPEAT-PASS L-BAND SAR INTERFEROMETRY OVER SPARSE VEGETATION COVERED REGIONS

Yang Lei[1], Cunren Liang[2], Jiancheng Shi[1], Charles Werner[3], Jing Zhang[1]

[1]National Space Science Center (NSSC), Chinese Academy of Sciences (CAS)
[2]Peking University
[3]GAMMA Remote Sensing AG

Background: Repeat-pass InSAR approach

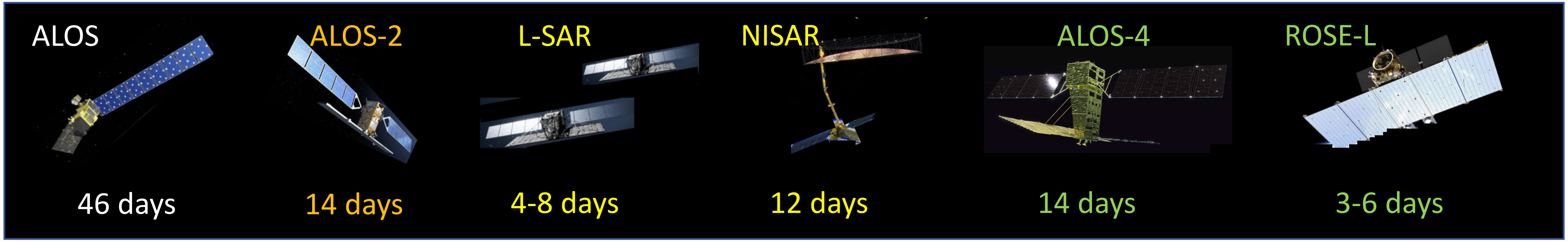

Problems:

For spaceborne L-band InSAR observations with long temporal baseline (tens of days to few months), temporal decorrelation dominates (especially when covered by vegetation) and phase unwrapping becomes problematic!

Motivation:

Given large archive of spaceborne L-band repeat-pass InSAR dataset, e.g. JAXA's ALOS, ALOS-2, future ALOS-4 , China's L-SAR, NASA's future NISAR, ESA's future ROSE-L, it is desired to refine the approach for such spaceborne L-band low-coherence dataset with long temporal baselines (tens of days to few months) and study the effect of sparse vegetation cover on SWE retrieval.

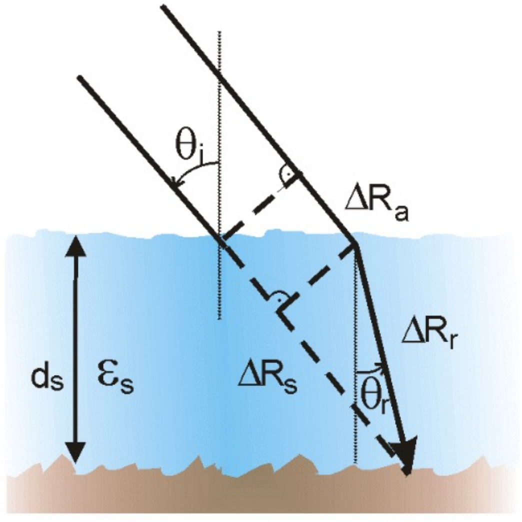

Credit: Rott et al., 2003

Methodology: InSAR Processing Workflow

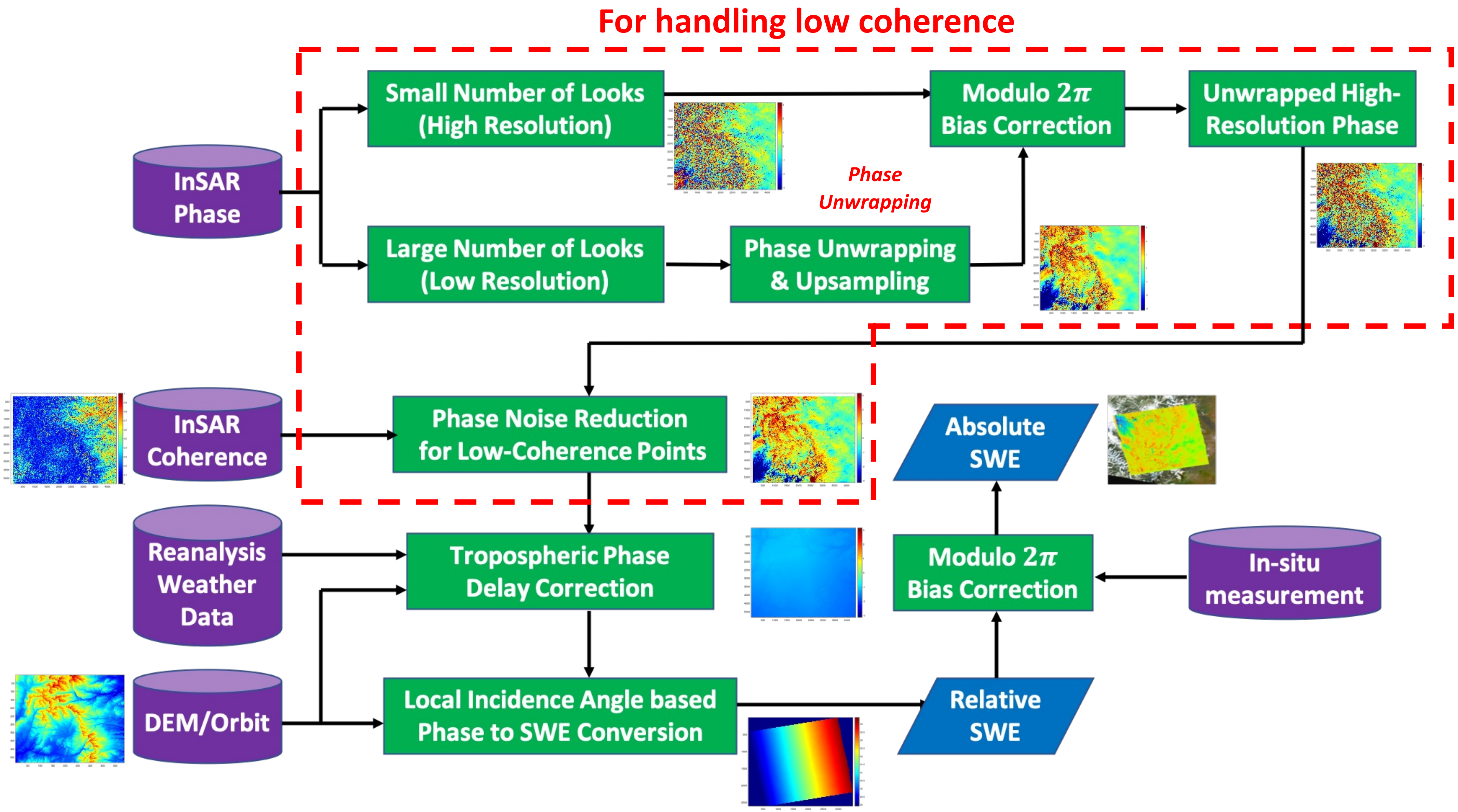

Methodology: InSAR scattering model

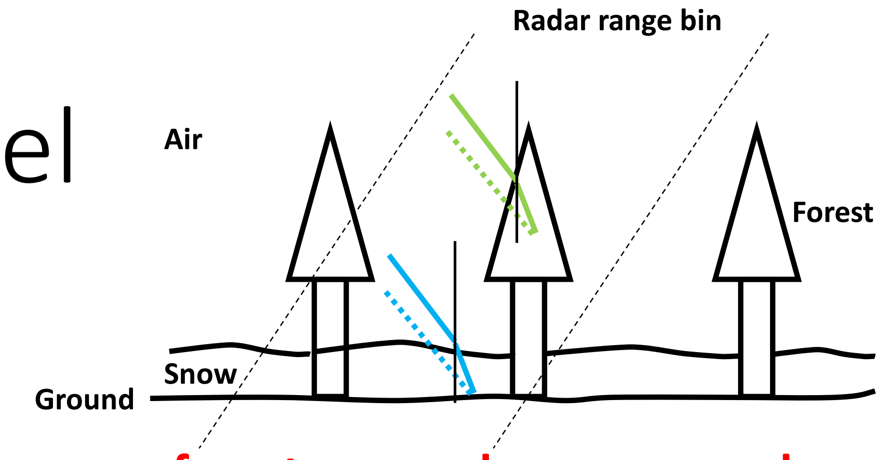

Snow-covered ground without vegetation

$$\Delta\Phi_s = 2k_i \cdot \frac{\alpha}{2}\left(1.59 + \theta^{5/2}\right) \cdot \Delta SWE$$

(Guneriussen et al., 2001; Leinss et al., 2015)

Physical repeat-pass InSAR scattering model for forest over ground (Lei et al., 2017)

$$\gamma = e^{j\phi_0}\frac{\gamma_{v\&t} + \gamma_d^g m}{1+m}$$

where

Dielectric Fluctuation

Random Motion

$$\begin{cases} \gamma_{v\&t} = \dfrac{\int_0^{h_v} \gamma_d^v(z)\rho_r(z)\bar{\sigma}_v(z)e^{-j\kappa_z z}dz}{\int_0^{h_v}\bar{\sigma}_v(z)dz} \\ m = \dfrac{\sqrt{G_1 G_2}}{\int_0^{h_v}\bar{\sigma}_v(z)dz} \\ \bar{\sigma}_v(z) = \sqrt{\sigma_1(z)\sigma_2(z)} \end{cases}$$

For modeling sparse forest-covered snow ground

Modified repeat-pass InSAR scattering model for forest over snow-covered ground

$$\gamma = e^{j\phi_0}\frac{\gamma_{v\&t} + \gamma_d^g m \boxed{e^{j\Delta\phi_g}}}{1+m}$$

Ground Phase Change → Guneriussen et al., 2001

where

Vegetation Phase Change → Snow cover increases effective dielectric constant of forest canopy

$$\begin{cases} \gamma_{v\&t} = \dfrac{\int_0^{h_v} \gamma_d^v(z)\rho_r(z)\bar{\sigma}_v(z)\boxed{e^{j\Delta\phi_v(z)}}e^{-i\kappa_z z}dz}{\int_0^{h_v}\bar{\sigma}_v(z)dz} \\ m = \dfrac{\sqrt{G_1 G_2}}{\int_0^{h_v}\bar{\sigma}_v(z)dz} \\ \bar{\sigma}_v(z) = \sqrt{\sigma_1(z)\sigma_2(z)} \end{cases}$$

Lei, Y., Siqueira, P. and Treuhaft, R., 2017. A physical scattering model of repeat-pass InSAR correlation for vegetation. *Waves in Random and Complex Media*, *27*(1), pp.129-152.

Methodology: model simulation

Snow-covered ground without vegetation

$$\Delta\Phi_s = 2k_i \cdot \frac{\alpha}{2}\left(1.59 + \theta^{5/2}\right) \cdot \Delta SWE$$

(Guneriussen et al., 2001; Leinss et al., 2015)

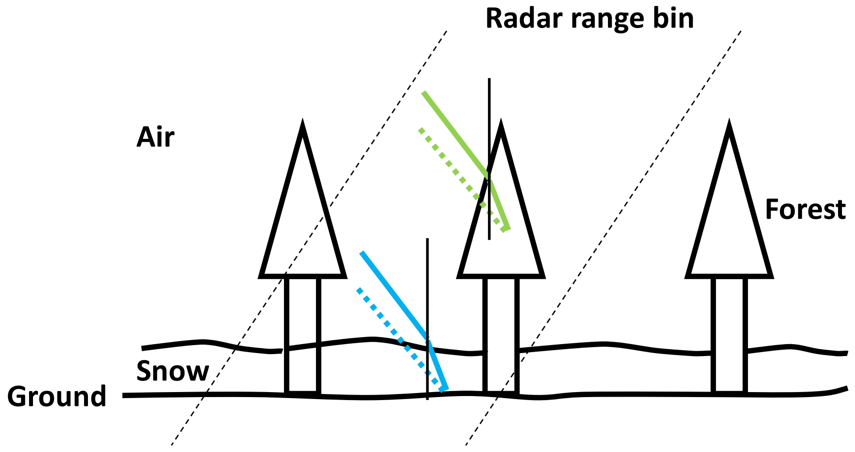

For modeling sparse forest-covered snow ground

Modified repeat-pass InSAR scattering model for forest-covered snow

$$\gamma = e^{j\phi_0} \frac{\gamma_{v\&t} + \gamma_d^g m \boxed{e^{j\Delta\phi_g}}}{1+m}$$

Ground Phase Change

where

Vegetation Phase Change

$$\begin{cases} \gamma_{v\&t} = \dfrac{\int_0^{h_v} \gamma_d^v(z)\rho_r(z)\bar{\sigma}_v(z)\boxed{e^{j\Delta\phi_v(z)}}e^{-i\kappa_z z}dz}{\int_0^{h_v}\bar{\sigma}_v(z)dz} \\ m = \dfrac{\sqrt{G_1 G_2}}{\int_0^{h_v}\bar{\sigma}_v(z)dz} \\ \bar{\sigma}_v(z) = \sqrt{\sigma_1(z)\sigma_2(z)} \end{cases}$$

Simulation setup

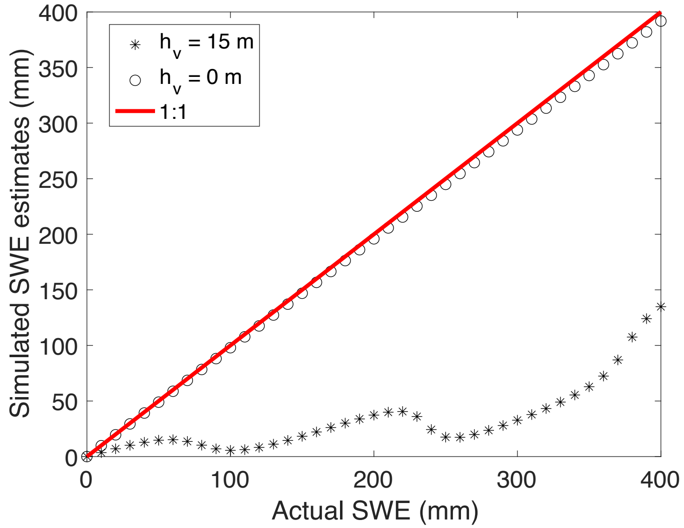

- $h_v = 15$ m
- Vegetation extinction coefficient of 0.1 dB/m
- Ground-to-volume ratio of -5 dB (for 15 m tall trees at L-band HH-pol; Pardini et al., 2021)
- $\gamma_d^v = \gamma_d^g = 0.7$
- Random motion of 2 cm for tree components at a reference height of 15 m
- Fixed snow density of 0.2 g/cm^3
- $\kappa_z = 0.01$ rad/m, $\lambda = 24.2$ cm, $\theta = 31.7°$ (for ALOS-2)
- Effective dielectric constant for snow-covered vegetation, ε_{veg}, assuming 1 cm increase of SWE causes ε_{veg} to increase by 3.2500e − 04

Study Area and Dataset

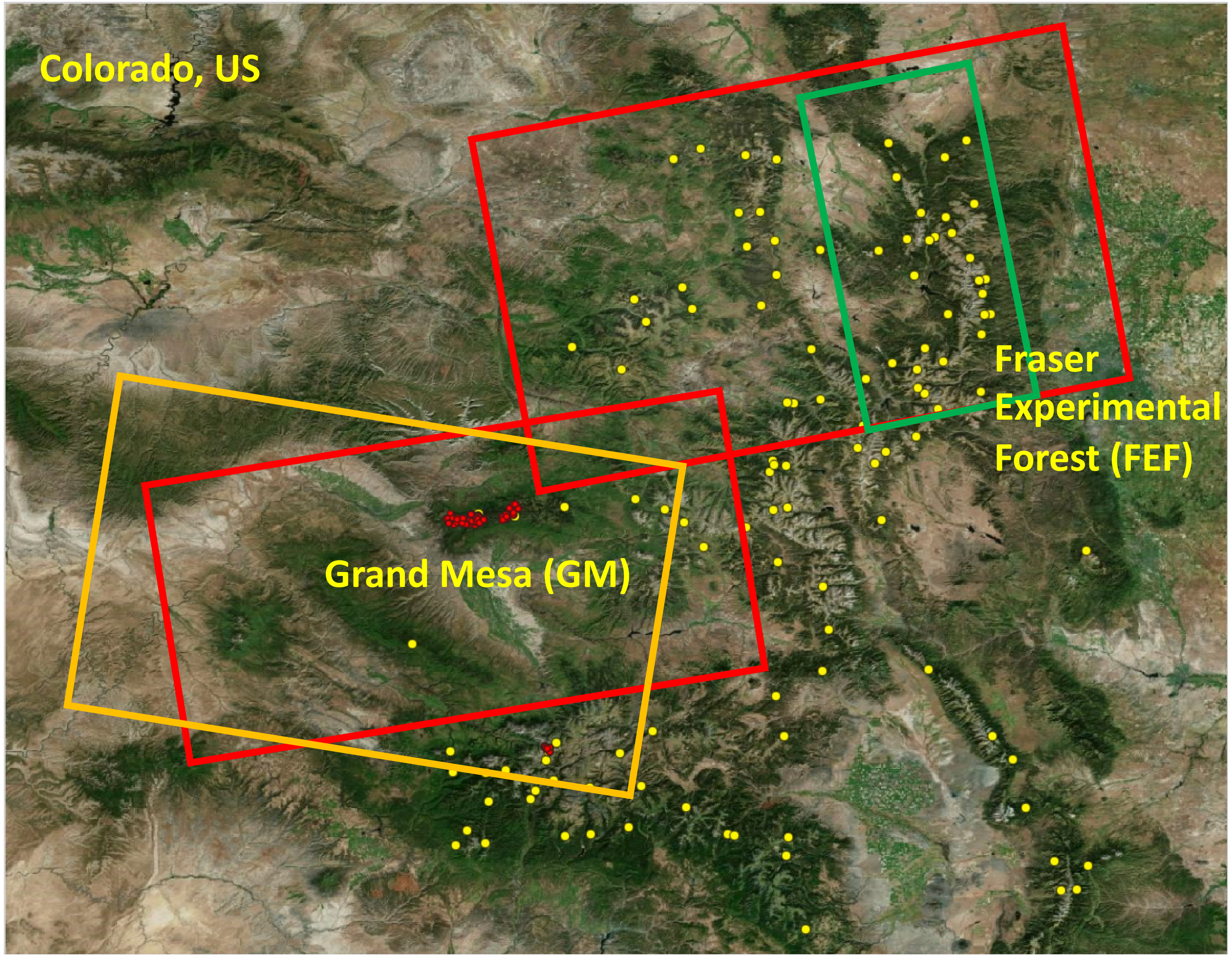

- SNOTEL weather stations (114 stations statewide; daily 1978-present)
- SnowEx 17 snow pit measurements (264 points; February 1-25, 2017)
- ALOS-2 stripmap FBD (3 scene mosaic; 20160912-20170130)
- Sentinel-1 TOPS ascending (1 scene; monthly 2016-2017)
- Sentinel-1 TOPS descending (1 scene; monthly 2016-2017)

GEDI-measured Sparse/short vegetation height: 10-20 m (average of 15 m)

Data Processing

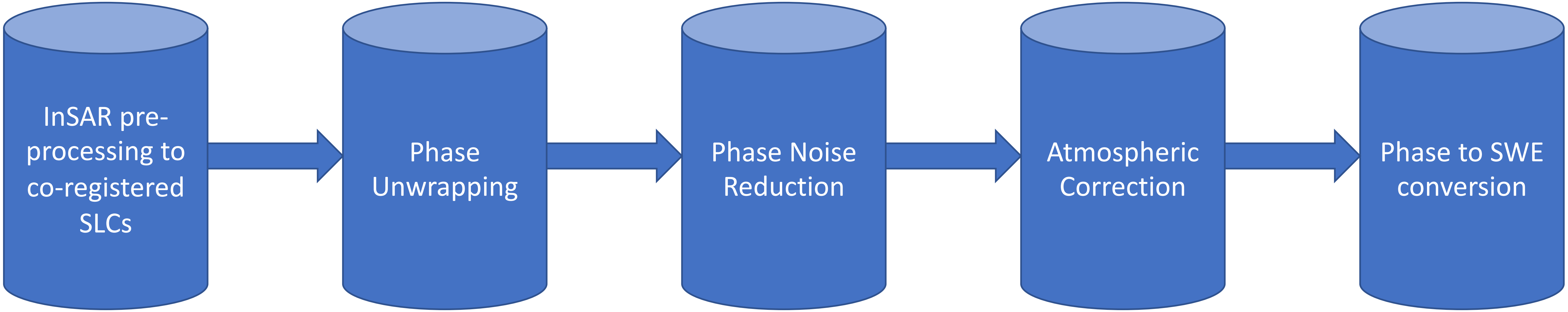

I. Phase Unwrapping

$$\phi_{\text{coarse}} = \phi_{\text{fine}} + m \cdot 2\pi + \varepsilon$$
$$\varepsilon \in [-\pi, \pi]$$

Solution

$$\varepsilon = (\phi_{\text{coarse}} - \phi_{\text{fine}}) - \text{round}\left[\frac{\phi_{\text{coarse}} - \phi_{\text{fine}}}{2\pi}\right] \cdot 2\pi$$
$$m = \frac{\phi_{\text{coarse}} - \phi_{\text{fine}} - \varepsilon}{2\pi}$$
$$\phi^* = \phi_{\text{fine}} + m \cdot 2\pi$$

Wrapped InSAR phase (2 rlks x 4 alks)

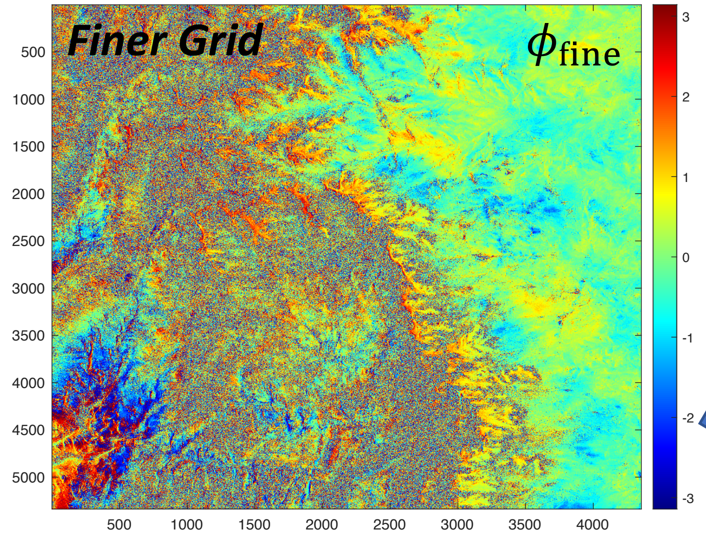

Unwrapped InSAR phase (12 rlks x 24 alks)

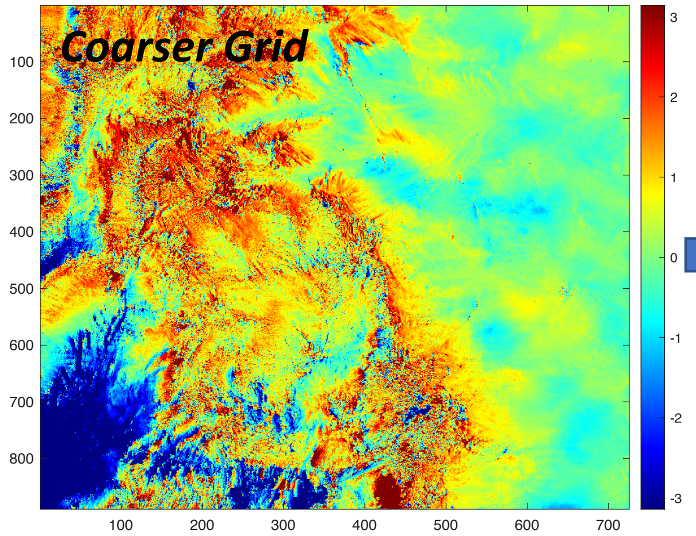

Interpolation to finer grid

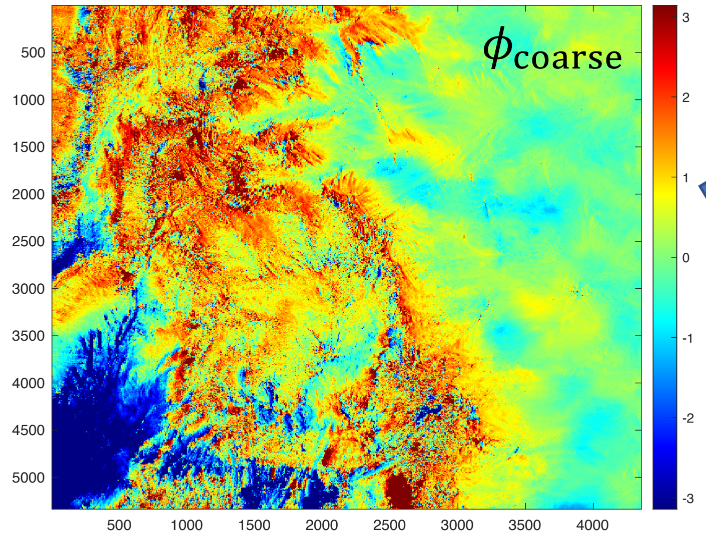

Unwrapping finer-grid phase with the coarser-grid reference

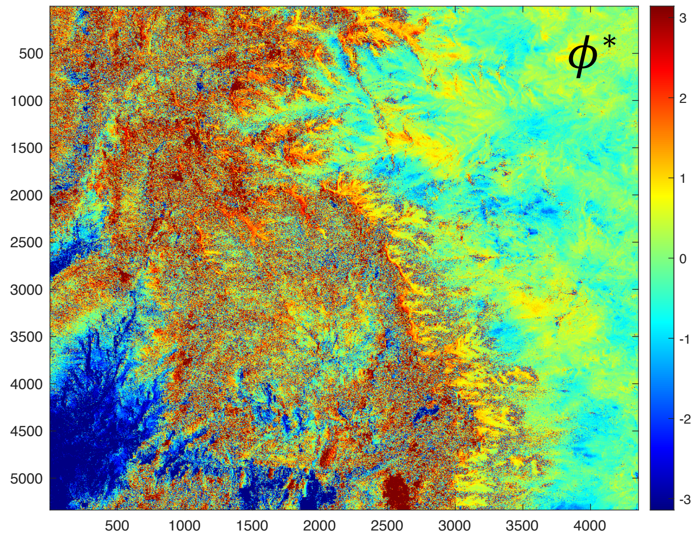

II. Phase Noise Reduction

Unwrapped InSAR phase (corrected)

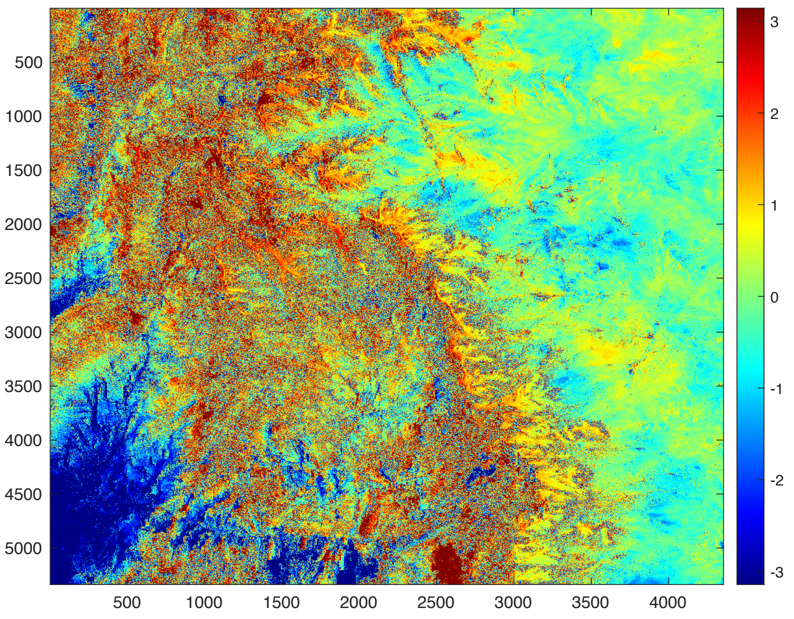

11 x 11 median filter

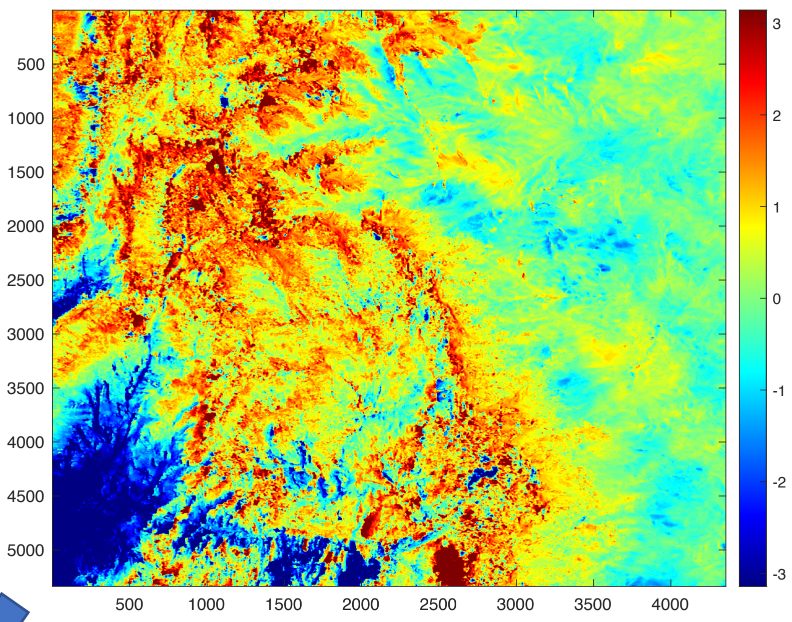

InSAR coherence

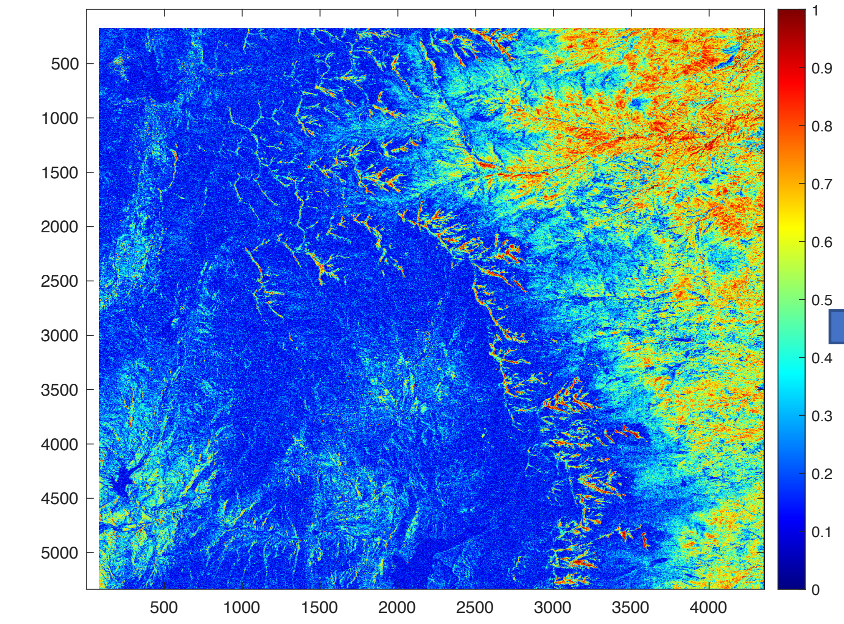

High-coherence unwrapped InSAR phase

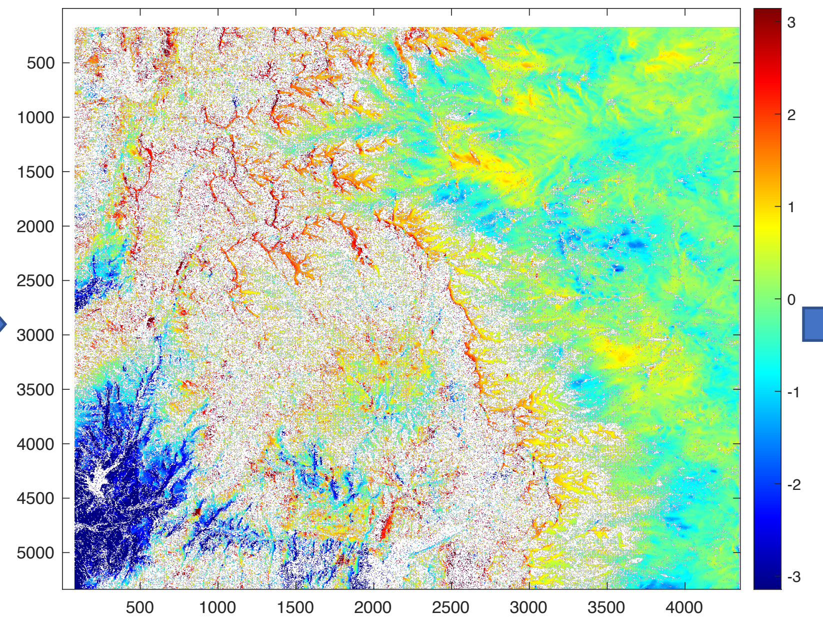

Interpolated phase

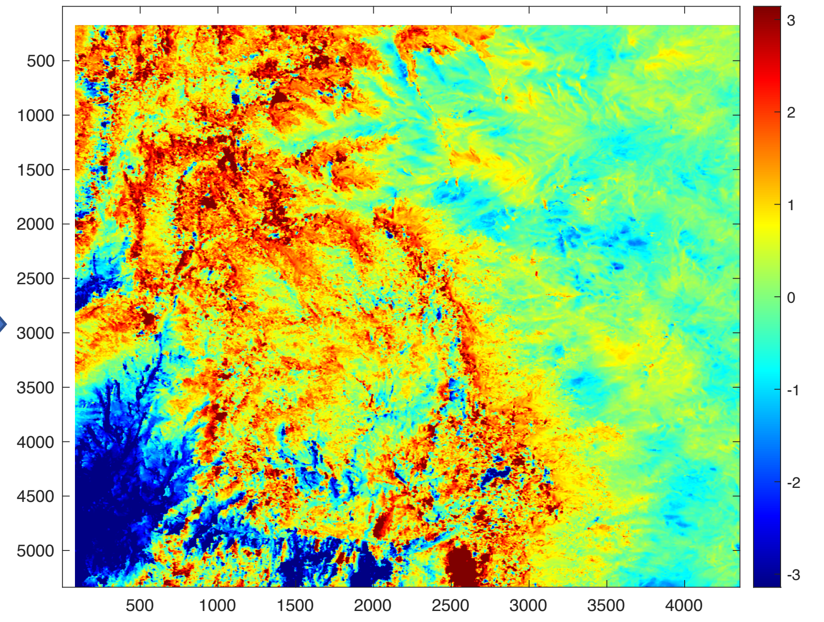

III. Troposphere Delay Correction

ERA-5 Reanalysis Weather Data

Troposphere phase delay (20160912)

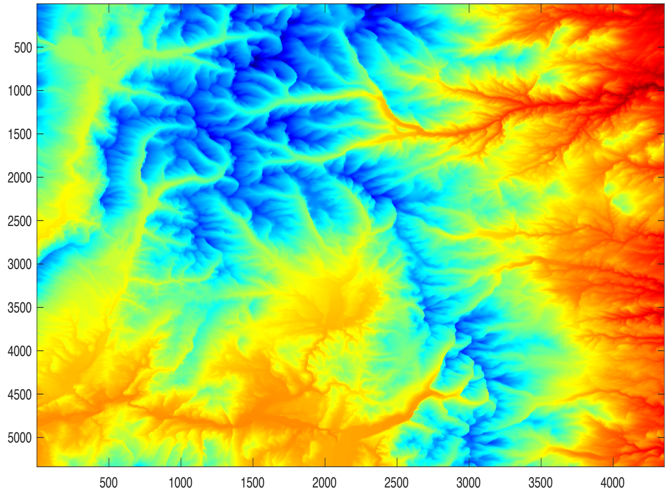

Troposphere phase delay (20170130)

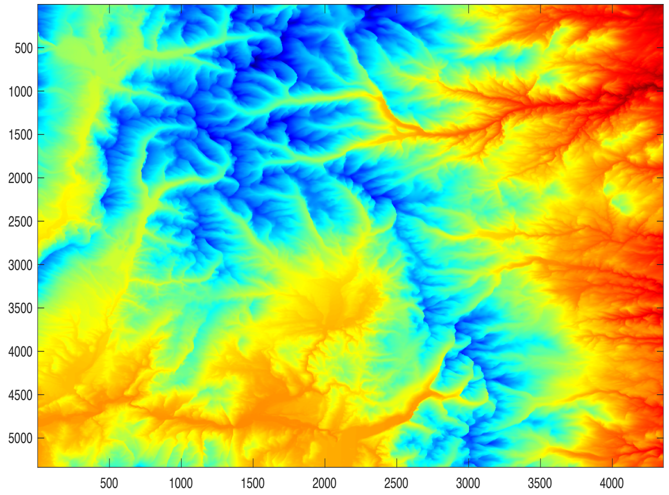

Tropospheric InSAR (differential) phase delay

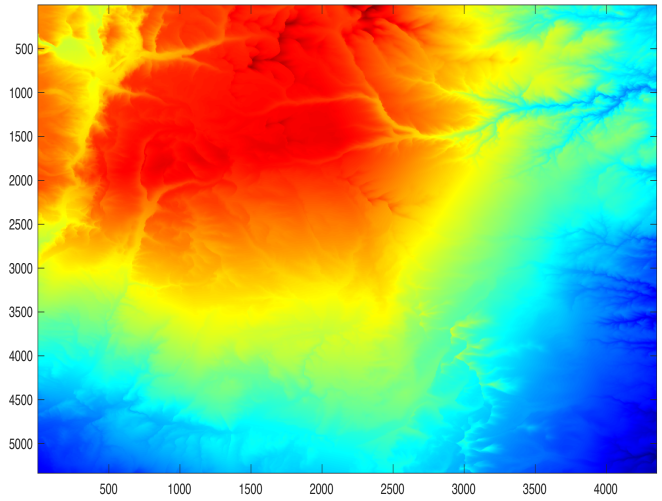

SRTM DEM

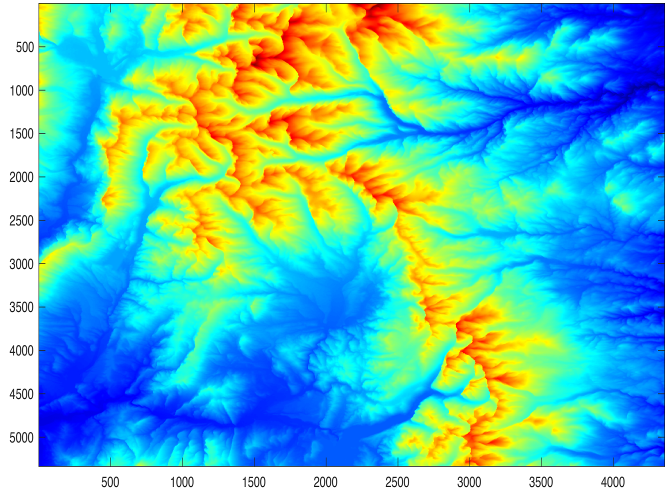

IV. Phase to SWE Conversion

Conversion Factor

$$\Delta\Phi_s = \boxed{2k_i \cdot \frac{\alpha}{2}\left(1.59+\theta^{5/2}\right)} \cdot \Delta\mathrm{SWE}.$$

Leinss et al., 2015

DEM derived
local incidence angle

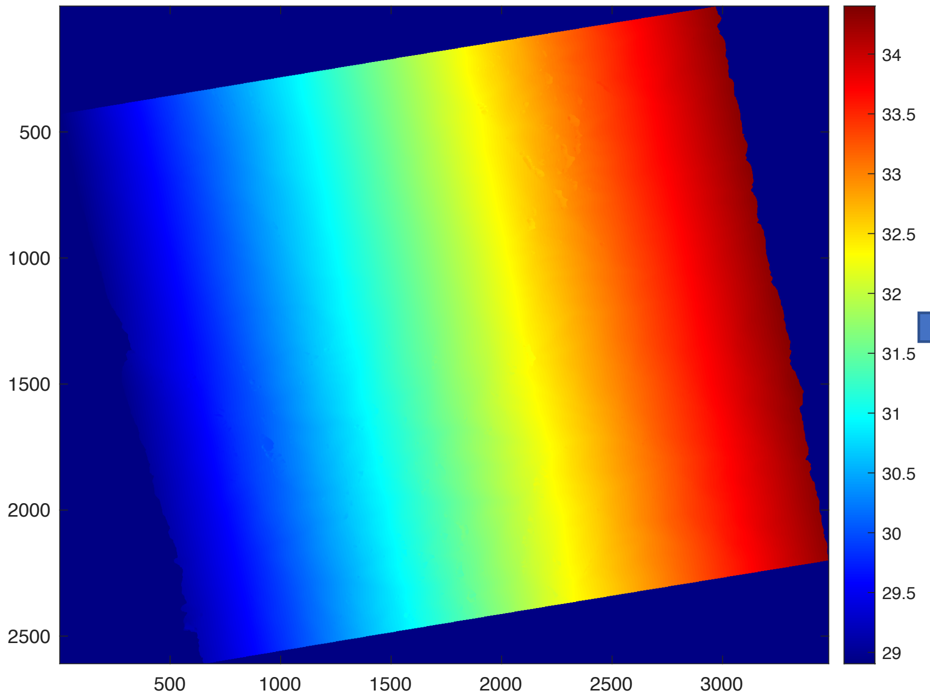

InSAR phase to SWE
conversion factor

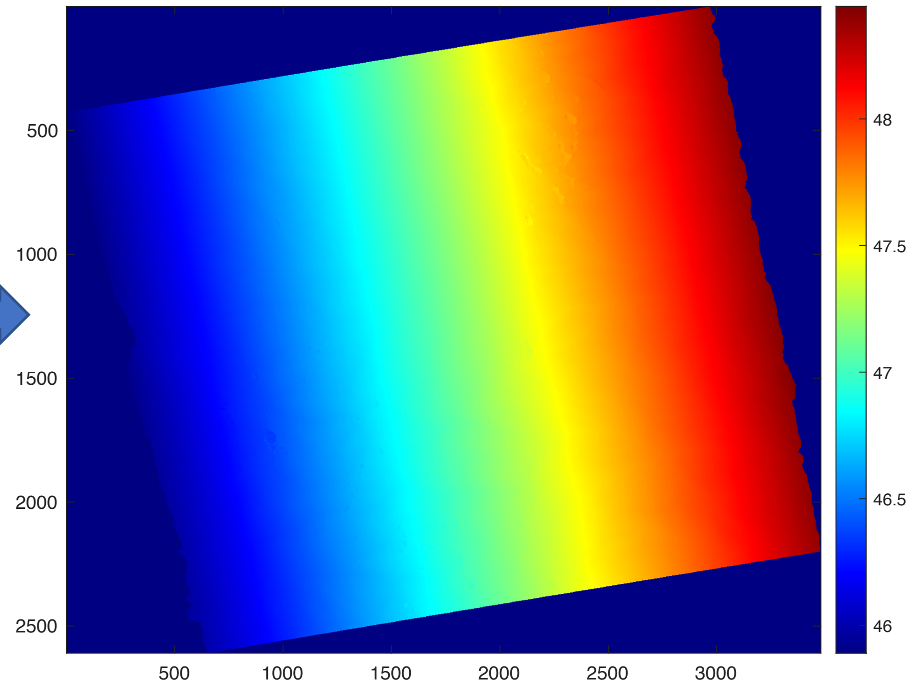

Validation of SWE product

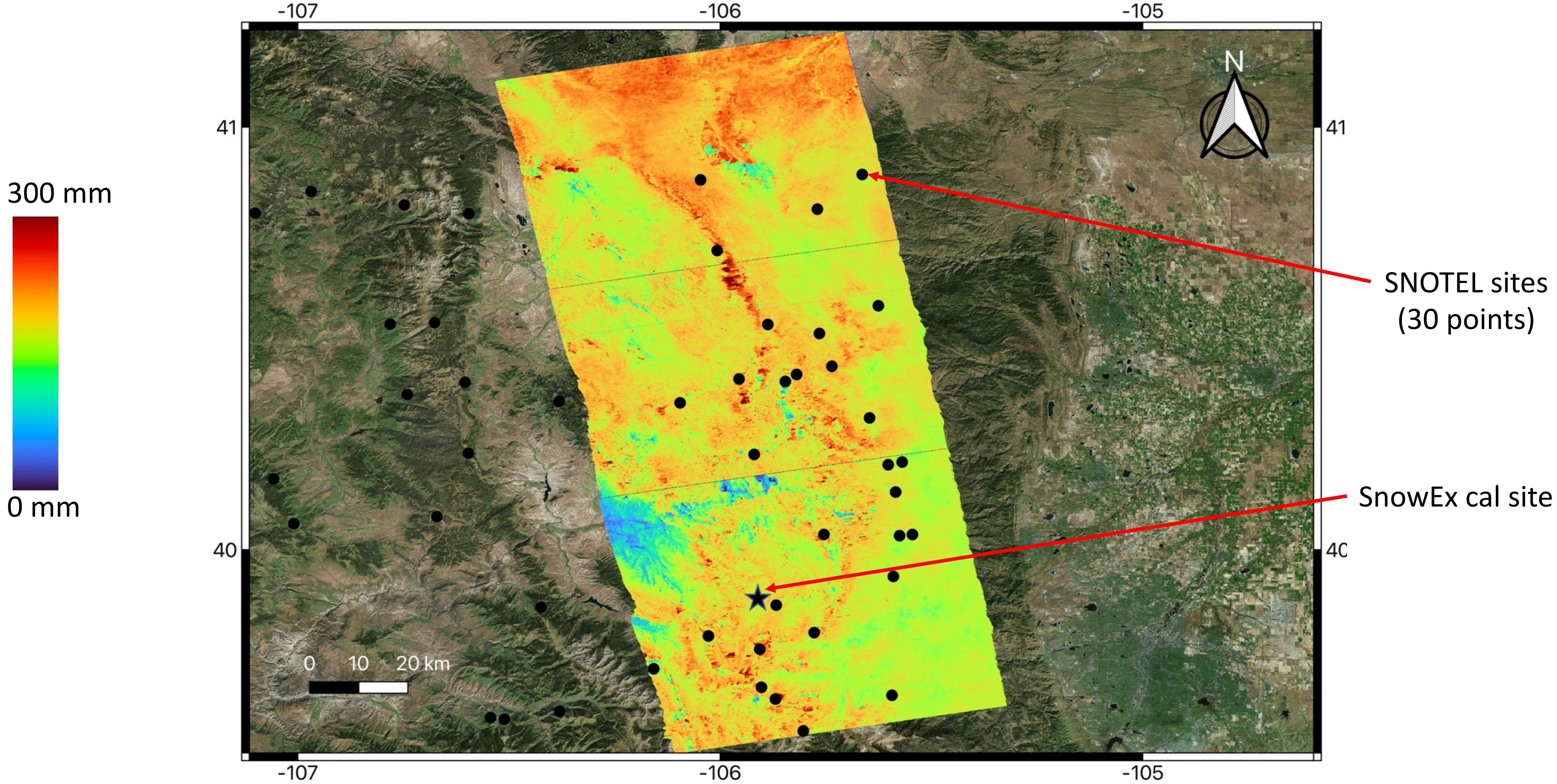

Comparison with optical image

SnowEx cal site

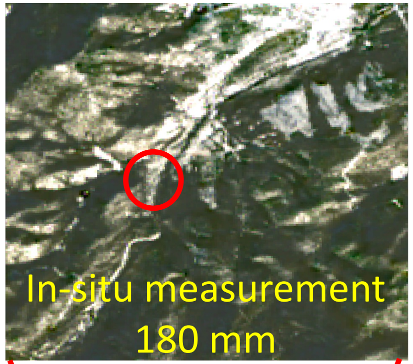

InSAR measurement
176 mm

InSAR Estimated SWE (mm)

300 mm

0 mm

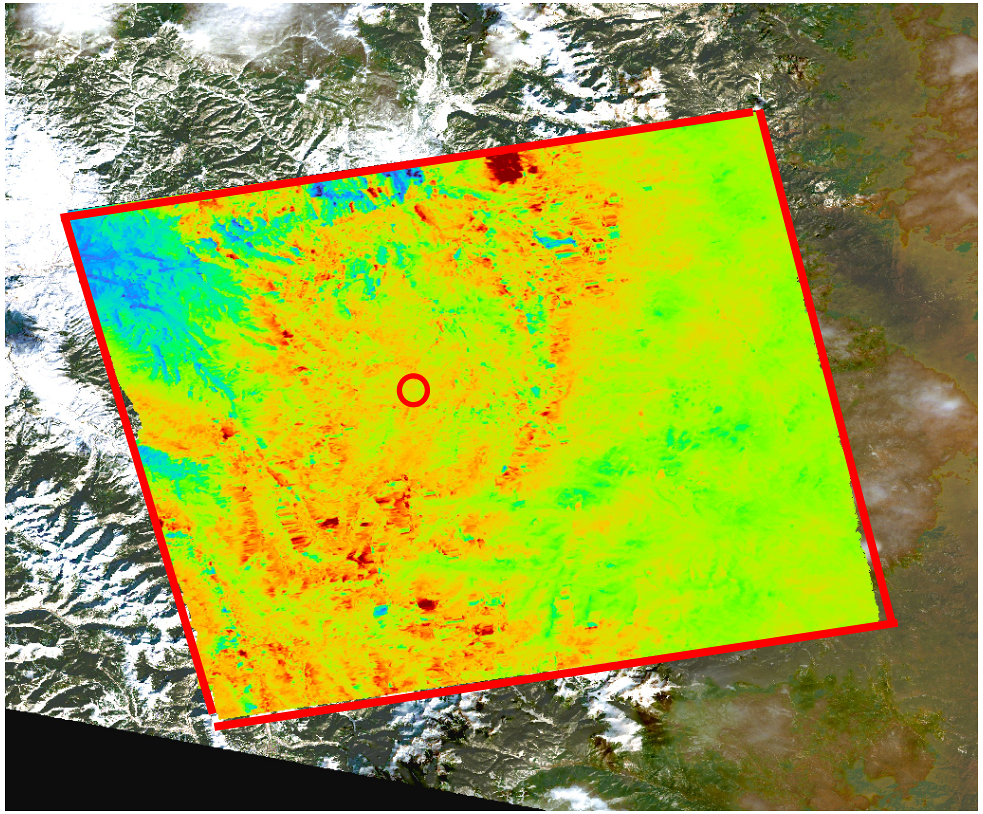

Landsat (20170131)

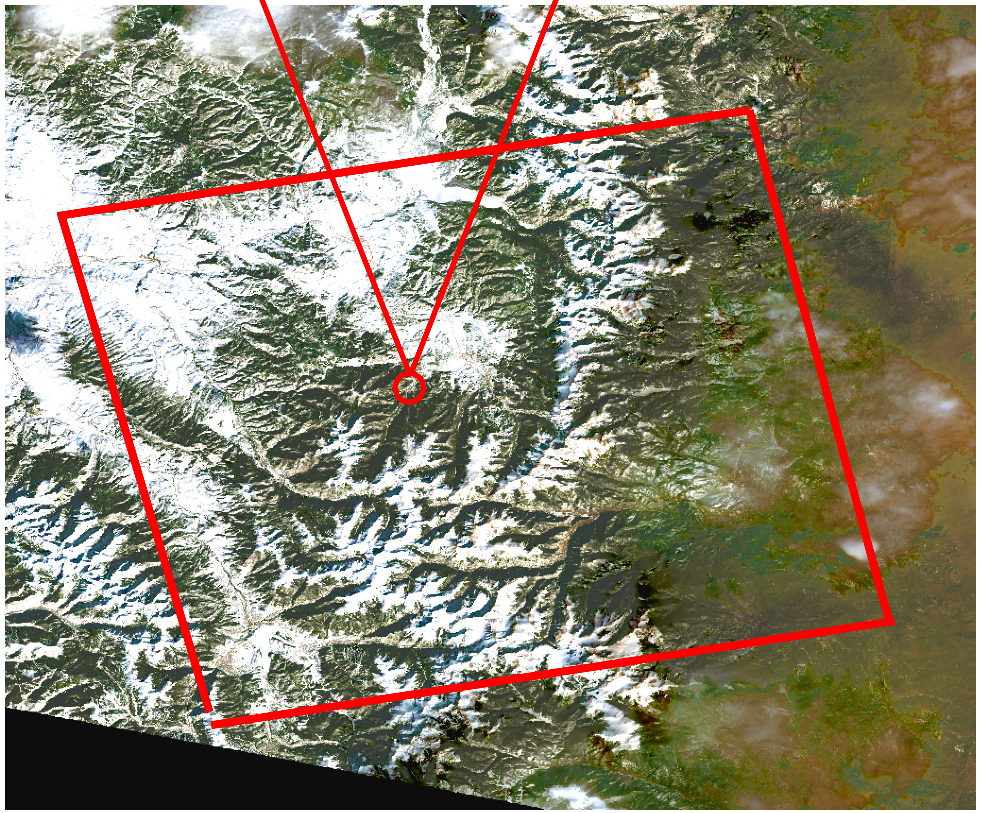

Comparison with SNOTEL in-situ data

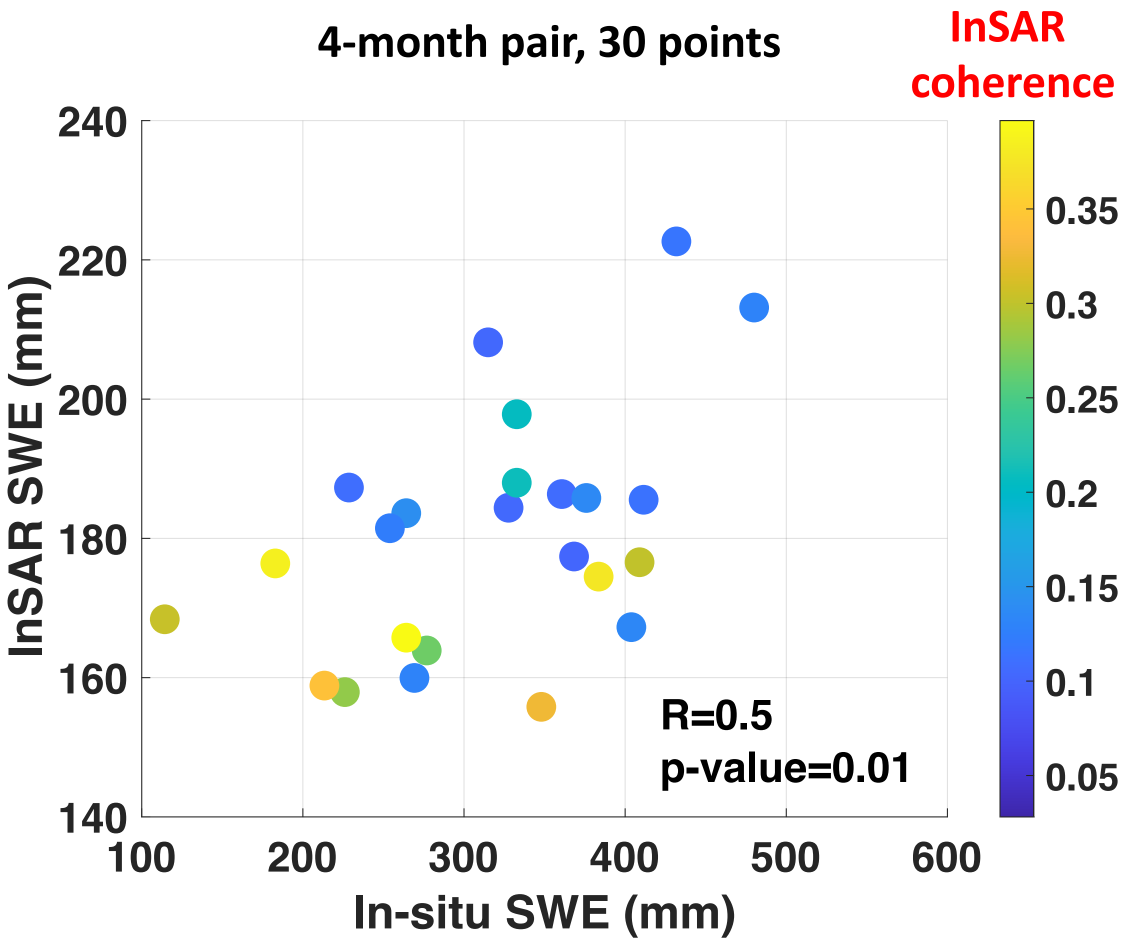

- Statistically significant correlation between the two dataset
- Large uncertainty due to temporal decorrelation with long temporal baseline (4 months)
- Short dynamic range of inversion results (80 mm) compared to in-situ measurements (400 mm), which will be explained later

Sentinel-1 C-band results

- ➢ Statistically significant correlation
- ➢ Smaller uncertainty due to shorter temporal baseline (6-12 days); longer temporal baseline decorrelates C-band signals rapidly over vegetated areas
- ➢ Even shorter dynamic range of SWE inversion results

Sentinel-1 9 points (ascending 6-day pair)

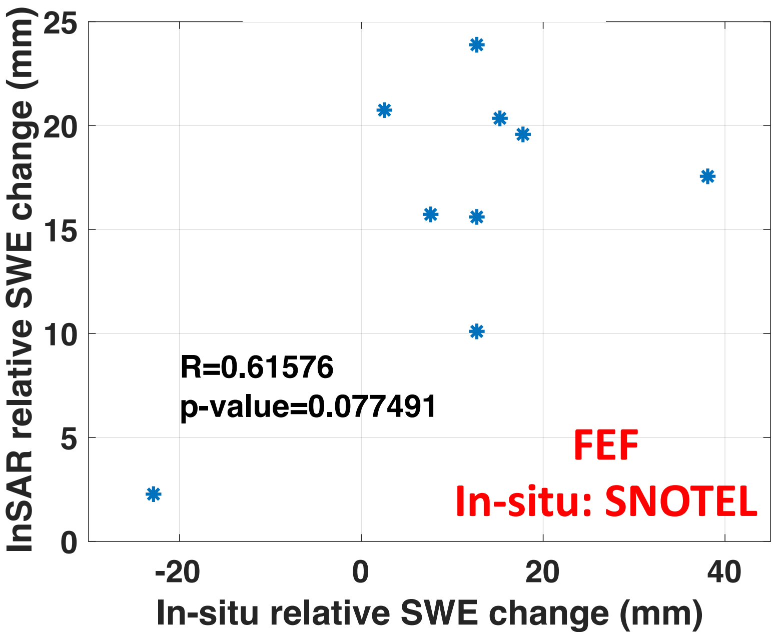

Sentinel-1 13 points (descending 12-day pair)

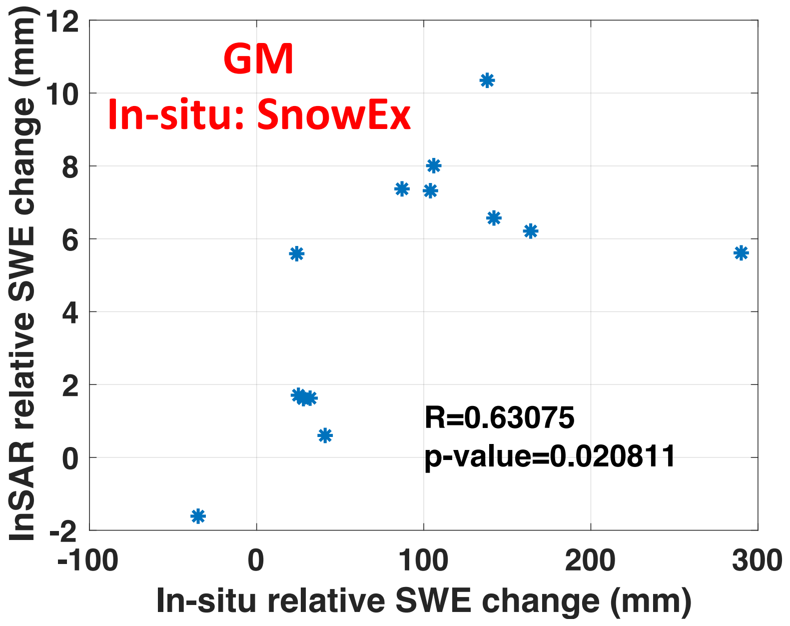

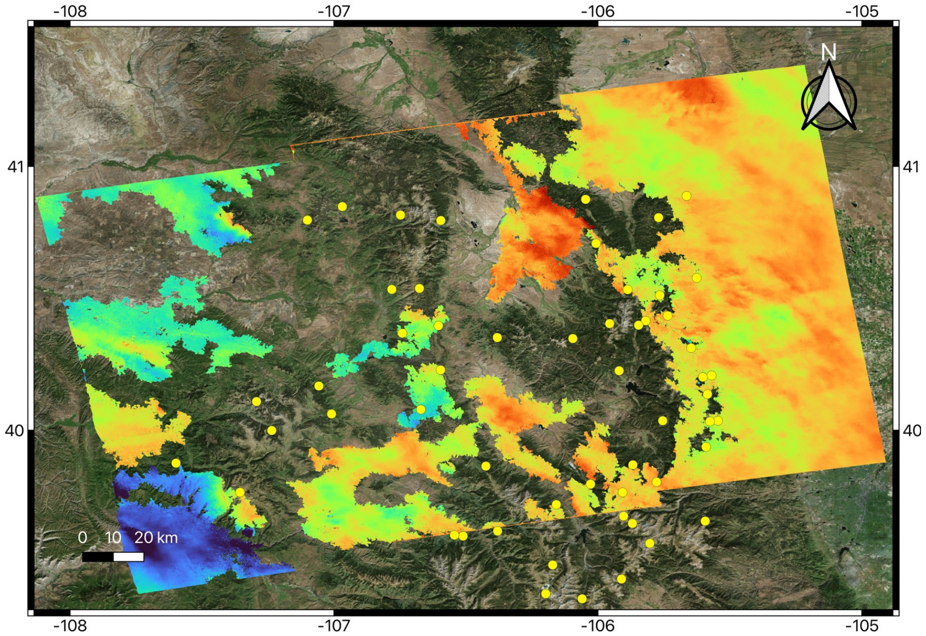

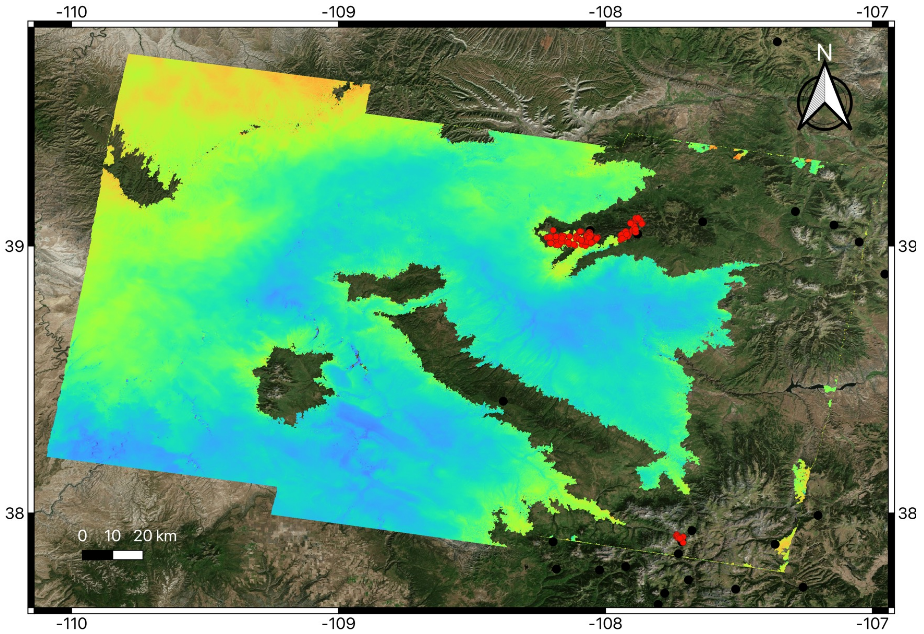

Conclusions

- L-band InSAR has promising performance with small but usable coherence (>0.2) even with a temporal span of 4 months
- Large uncertainty of L-band InSAR can be reduced a lot when using shorter temporal spans e.g. 12 days for NISAR or 4-8 days for China's L-SAR
- C-band InSAR has poor coherence with a temporal span of >=6 days when subjected to vegetation-dominated temporal decorrelation
- L-band InSAR phase affected by sparse vegetation scattering result in smaller dynamic range of inverted SWE compared to no-veg covered case, C-band more severely affected
- Further experimental validation and model analysis are desired using shorter temporal baselines (< 1 month) at L-band over various forest conditions

Thanks!

Freeze/thaw soil analysis

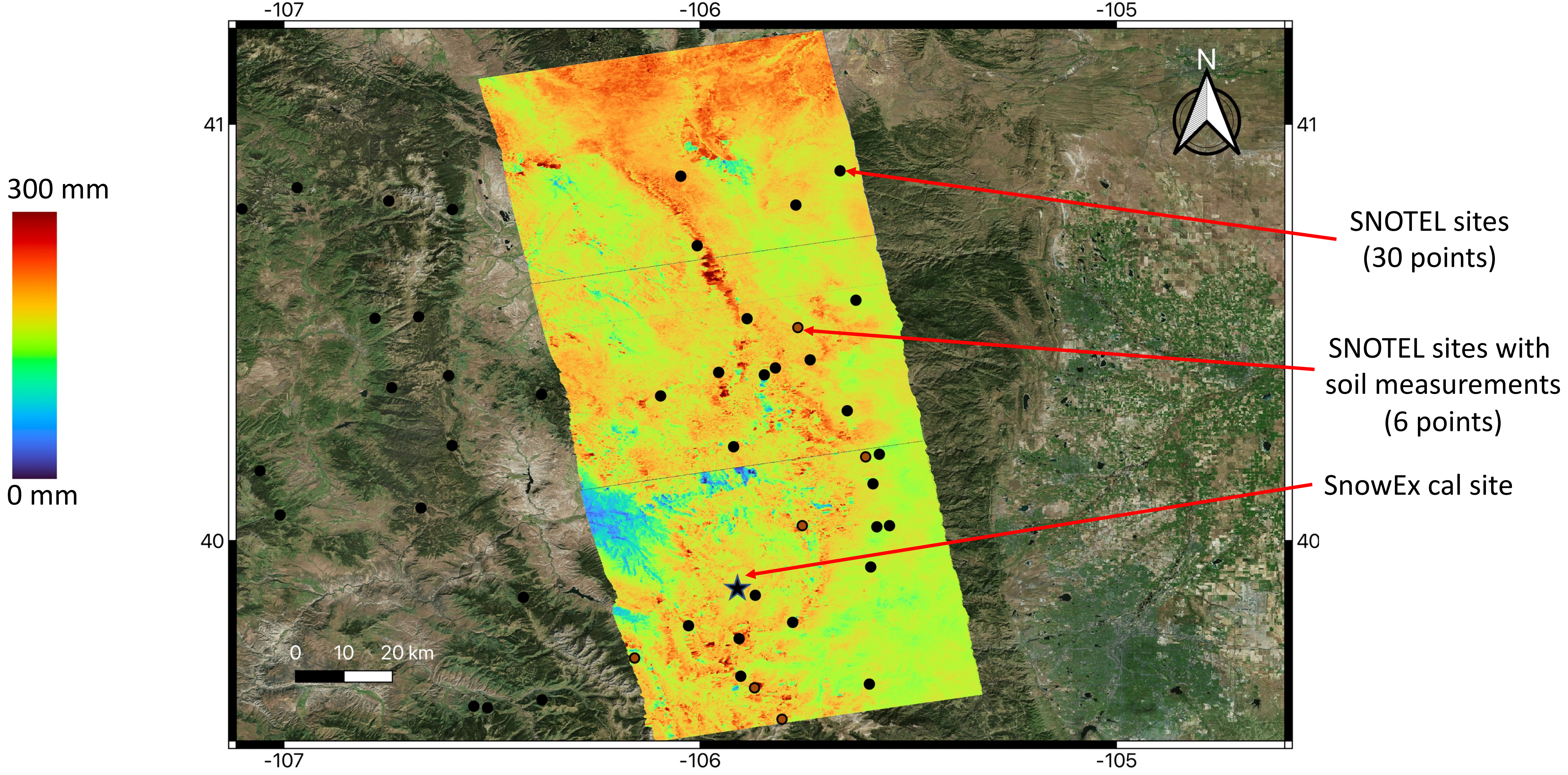

Freeze/thaw soil analysis

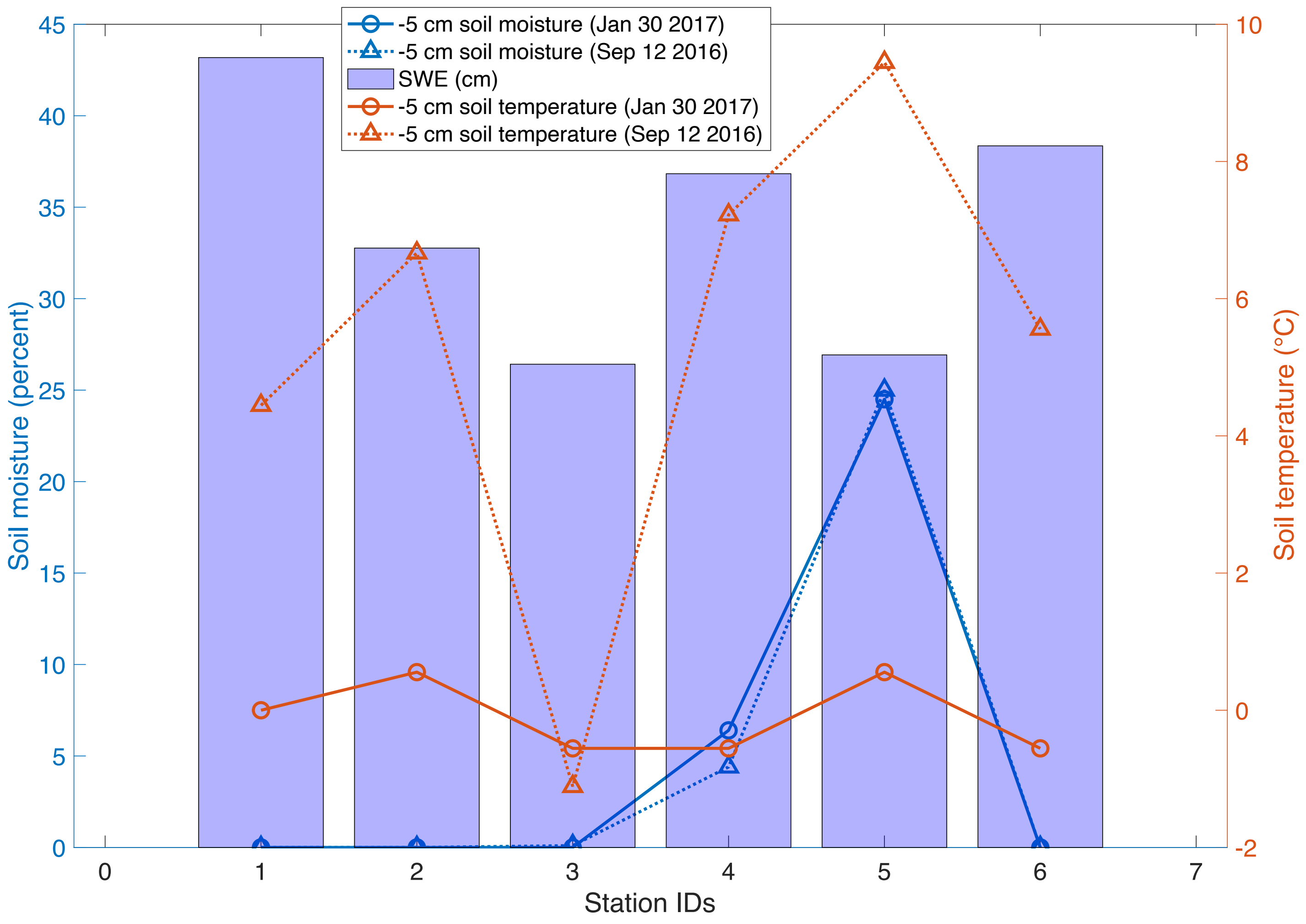

- Only 6 out of the 30 SNOTEL stations have soil condition measurements and they are evenly distributed across the study area (thus considered representative of the larger region)
- Dry soil with similar small moisture between the two dates of the InSAR pair
- For the single site with moisture of 25%, the temperature in winter was above zero (unfrozen)

Both the freeze/thaw induced deformation and penetration depth change are small here

The long-term freeze/thaw soil state change may introduce an overall bias of InSAR phase delay as well as increase the SWE inversion uncertainty (few-cm level phase delay), but does not account for the inverted SWE trend that correlates with in-situ SWE (tens of cm phase delay), which should be due to the snow accumulation